

# Decomposition Behavior of Kevlar 49 Fibers:

## Part II. At $T$ values $< T_d$

R. V. IYER

A. SUDHAKAR

KALYANI VIJAYAN<sup>1</sup>

*Materials Science Division, National Aerospace Laboratories, Bangalore 560017, India*

(Received 11 March 2004; accepted 5 January 2005)

**Abstract:** The residual effects of thermal aging of Kevlar 49 fibers in the temperature range 150–450°C have been analyzed. Thermal aging introduces crystallographic as well as macro-structural changes. Weight losses and deterioration in tensile properties were also observed. The order in which the deterioration in crystallinity, weight and tensile strength occur has been identified. Master curves for predicting the time needed for 50% deterioration at various temperatures and the corresponding activation energy have been estimated. The role of the parameter,  $t_{\text{cum}}(T)$ , the cumulative exposure to any temperature  $T$ , on thermally induced effects has been unambiguously established. In particular, the influence of the  $T-t_{\text{cum}}(T)$  effect on crystallographic parameters has been observed for the first time.

**Key Words:** Kevlar 49, structural changes, thermal aging, decomposition,  $T-t_{\text{cum}}(T)$  effect

### 1. INTRODUCTION

Kevlar fibers are reported to decompose at a  $T_d$  of approximately 500/550°C [1, 2]. In an earlier communication [3], details of the structural changes which accompany decomposition at 500 and 550°C were presented. It was shown that at both these temperatures, cumulative thermal exposures of specific durations,  $t_{\text{cum}}(T)$ , were required to cause decomposition. Decomposition was accompanied by prominent structural changes such as progressive reduction and an eventual total loss in crystallinity, progressive loss in weight, introduction of surface damage, hollowness and deterioration in tensile properties. Using these features as signatures of isothermal decomposition, the effect of thermal aging of Kevlar 49 fibers at  $T$  values  $< T_d$  have been analyzed and the details of this analysis are presented in this paper.

It must be mentioned that the behavior of Twaron fibers aged at 300, 400, 450, and 500°C has been earlier reported from our laboratory [4]. The tensile properties of the Twaron fibers used in the previous study were close to those of Kevlar 29 fibers. As such,

the investigation on Twaron fiber was, in principle, comparable to the study of Kevlar 29 fibers. The present investigation, on the other hand, was on Kevlar 49 fibers, which have better initial tensile properties.

## 2. EXPERIMENTAL DETAILS

The samples used were Kevlar 49 fibers made commercially available by DuPont Inc. USA. The temperatures ( $T$ ) chosen for thermal aging were 150, 250, 300, 350, 400 and 450°C. Of these, 150, 250, and 300°C are within the recommended service range of temperatures. For temperatures other than 150°C, a tubular resistance furnace in which a PID controller could control and maintain the temperature to an accuracy of  $\pm 1^\circ\text{C}$ , was used. For heating at 150°C, an air-circulating oven in which the control and stability of temperature was  $\pm 2^\circ\text{C}$  was used. Both prior to and at various stages of heat treatment, the fibers were characterized by X-ray diffraction methods, tensile testing, weight analysis, optical and scanning electron microscopy. Details of heating and the various procedures used for characterization have been described earlier [3–5]. For each of the characterization procedures, a separate bundle of fibers was heat treated. In addition to the surface characteristics, the cross-sectional features of some of the heat-treated fibers that fractured in tension were also examined using a scanning electron microscope. For fibers exposed to 150 and 250°C, the fracture was effected in an aqueous medium whereas for higher temperatures, the fibers had turned so brittle that transfer to the water medium led to an instant breaking. For these specimens, the tensile fracture was therefore carried out in air.

## 3. RESULTS AND DISCUSSION

Interestingly, the changes introduced by isothermal aging at  $T$  values  $< T_d$  closely resemble those accompanying exposures to  $T = 500$  and  $550^\circ\text{C}$  [5].

### 3.1. X-ray analysis

#### 3.1.1. Crystallinity

Figure 1 presents the equatorial diffraction profiles recorded from fibers isothermally aged in the temperature range 150–450°C. With the exception of 150°C, the general effect of isothermal aging is to reduce the initial crystallinity. For  $T$  values  $\geq 250^\circ\text{C}$ , values of residual crystallinity,  $K (= A/A_0)$  estimated from the integrated intensities of profiles in figure 1, are recorded in figure 2. Here  $A_0$  and  $A$  refer to the integrated intensities of the diffraction patterns recorded from fibers, prior to and after heat treatment, respectively. It may be noticed that 300 h of discontinuous yet cumulative thermal exposure to 300°C reduces the initial crystallinity by 80%. The effect of the parameters  $T$  and  $t_{\text{cum}}(T)$  can also

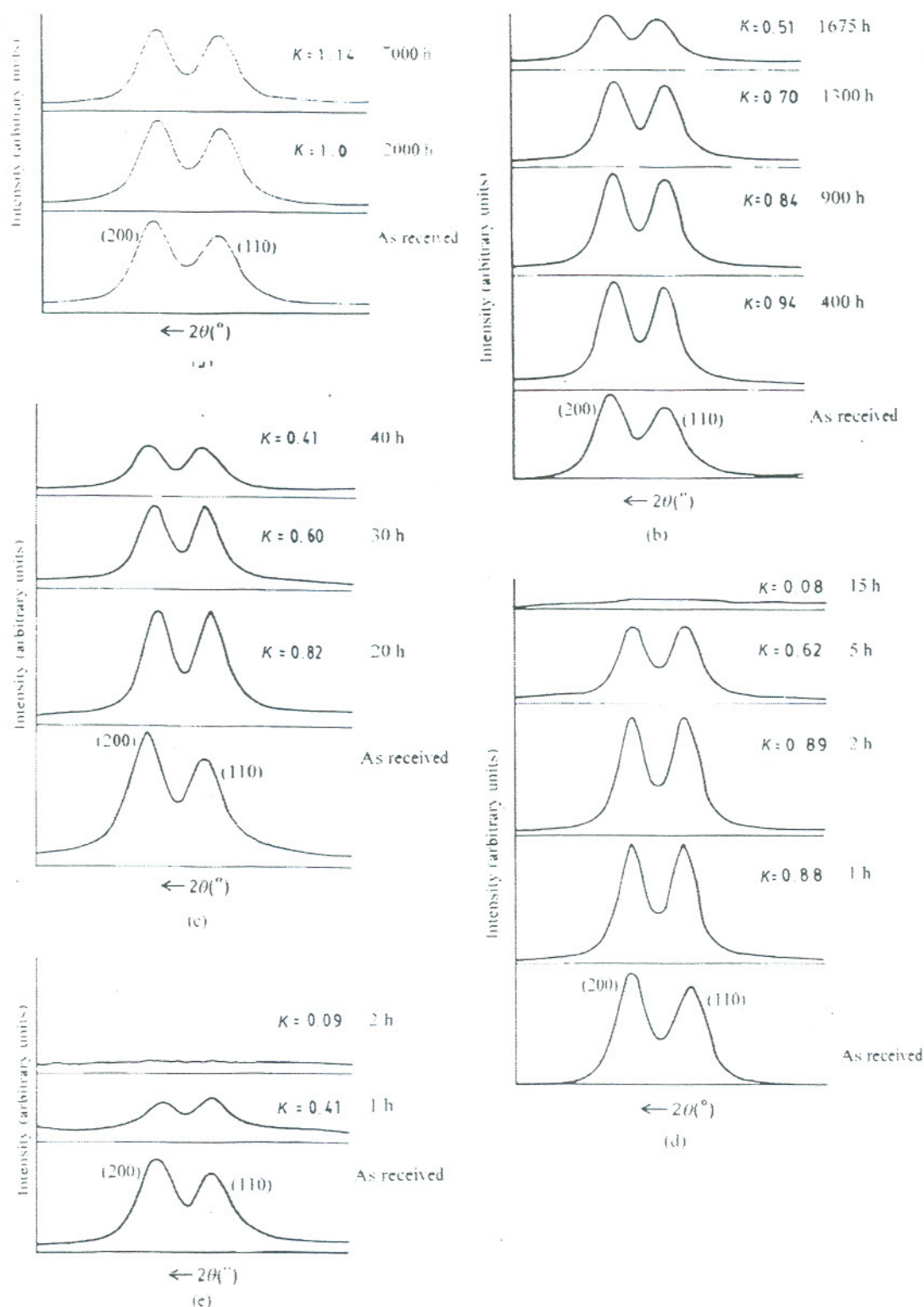


Figure 1. Diffraction profiles from fibers isothermally aged at (a) 150 (b) 250 (c) 350 (d) 400 and (e) 450°C. Values of  $K$  have also been shown.



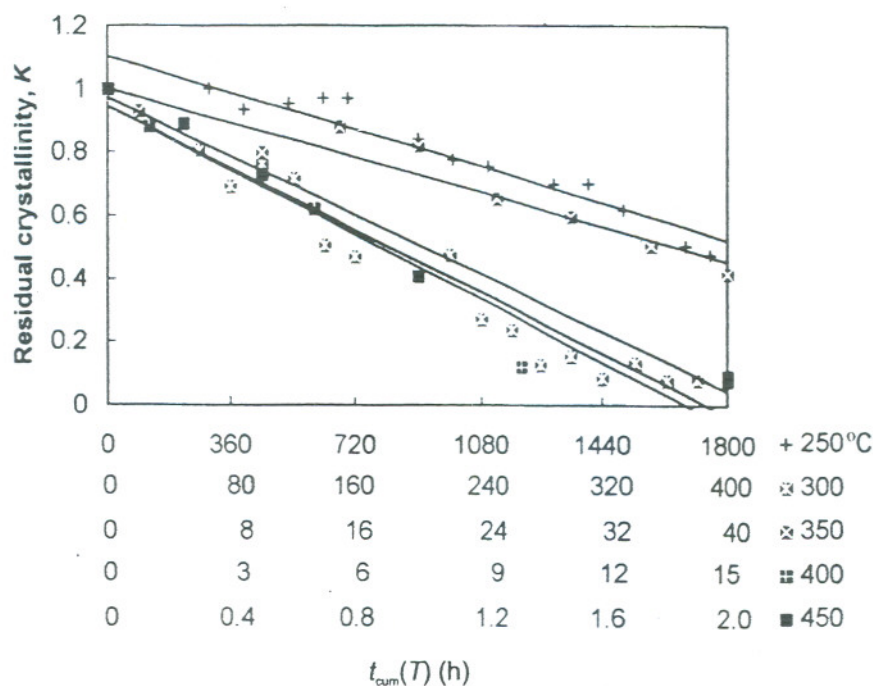


Figure 2. Residual crystallinity of fibers aged at  $T$  values of 250–450°C.

be appreciated from figure 2. An increase in the  $T$  as well as the  $t_{\text{cum}}(T)$  values enhances the reduction in crystallinity. Based on the above-mentioned X-ray data, the duration of cumulative exposure  $t_{0.5}$ , needed to introduce 50% reduction in the initial crystallinity, has been estimated (figure 3). For the sake of completion, data corresponding to 500, 550 and 600°C [5] have also been included in figure 3. It must be pointed out that the curve in figure 3 can be used to predict the residual crystallinity at any intermediate temperature also.

The activation energy  $E$  for 50% reduction in crystallinity was also obtained as 105.8 kJ mol<sup>-1</sup> from the Arrhenius equation

$$r = A \exp(-E/RT)$$

where  $r$  is the reaction rate constant derived from the  $t_{0.5}$  values,  $A$  is the pre-exponential factor and  $R$  is the gas constant. The master curve for predicting the changes in crystallinity over an extended time scale has also been generated by choosing 250°C as the standard temperature (figure 4). The procedure followed for generating the master curve is based on a constant energy model [6] according to which the activation energy is independent of temperature. The superposition shown in figure 4, although not ideal, is satisfactory. The reason for the slight fanning observed at the high end, namely for crystallinity values down to 0.7, is not clear at present.

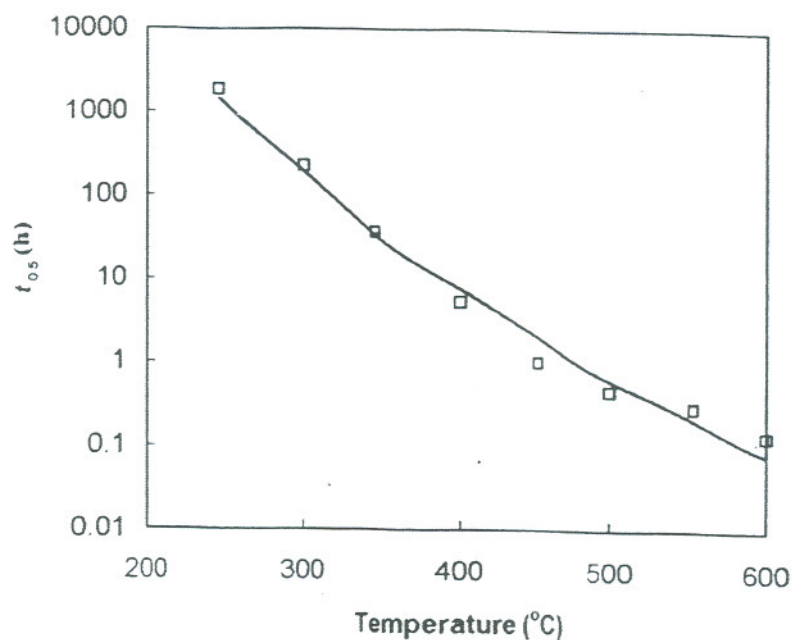


Figure 3. Time required for 50% reduction in crystallinity.

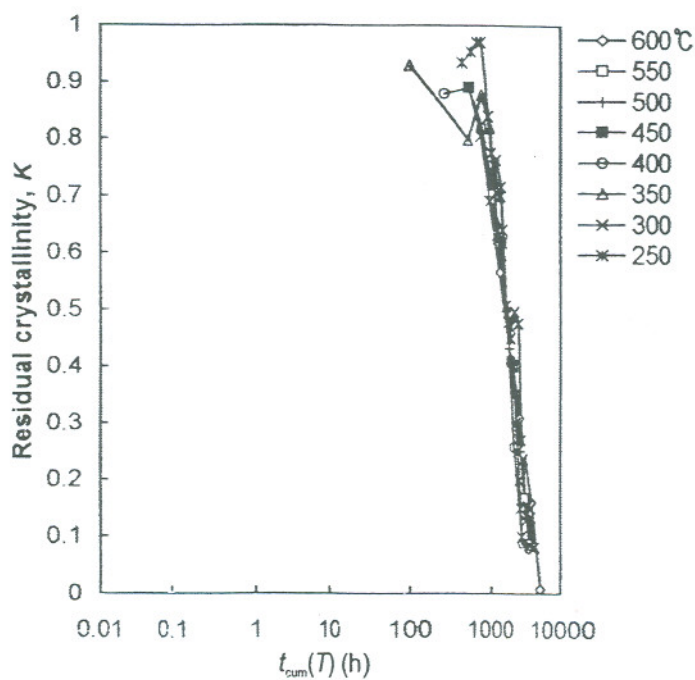


Figure 4. Master curve showing the variation of residual crystallinity: x-axis on log scale.

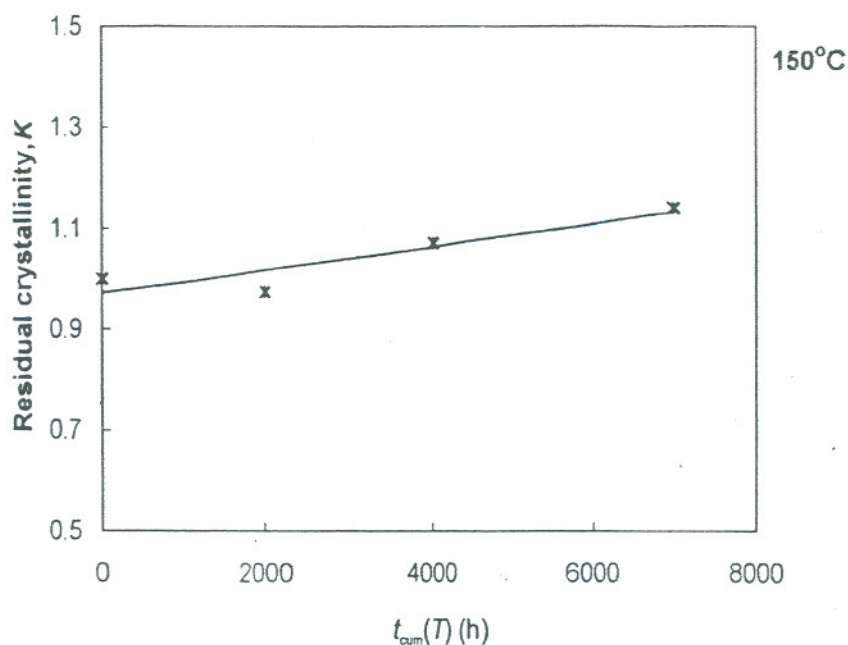


Figure 5. Variation of residual crystallinity with  $t_{\text{cum}}(T)$  at 150°C.

Interestingly, the behavior of crystallinity at 150°C is very different. As shown in figure 5, the crystallinity increases steadily with exposures of up to 7000 h duration. It must be mentioned that Hindeleh and Abdo also observed a similar increase in crystallinity at 150°C [7]. Their data, however, do not extend up to 7000 h. The present X-ray data thus suggest that 150°C is perhaps an ideal temperature for annealing and improving the crystallinity of commercially available Kevlar fibers.

### 3.1.2. $2\theta$ values

As in the case of Kevlar 49 fibers exposed to 500 and 550°C [3, 5]  $2\theta$  values of the equatorial reflections manifest the residual effects of exposure to  $T$  values in the range 150–450°C. Figure 6 depicts the observed variations in the  $2\theta$  values. The average value, 4.3, for the  $|\Delta|/\sigma$  of the  $2\theta$  values, establishes the statistical significance of the observations. Here,  $\Delta$  and  $\sigma$  refer to the observed shift accompanying thermal aging and the corresponding standard deviation respectively. It is found that both  $2\theta(200)$  and  $2\theta(110)$  values shift towards lower angles. The shifts in  $2\theta(200)$  are, however, much more than in  $2\theta(110)$ . Such an enhanced reduction in the  $2\theta(200)$  values may be attributed to the presence of van der Waal's interactions along the crystallographic  $a$ -direction, which is also the direction along which the hydrogen-bonded layers are stacked [8]. The observed shifts suggest that thermal aging weakens the inter-layer interactions in the crystal structure. The striking feature, however, is the initial non-linear dependence of the shifts on



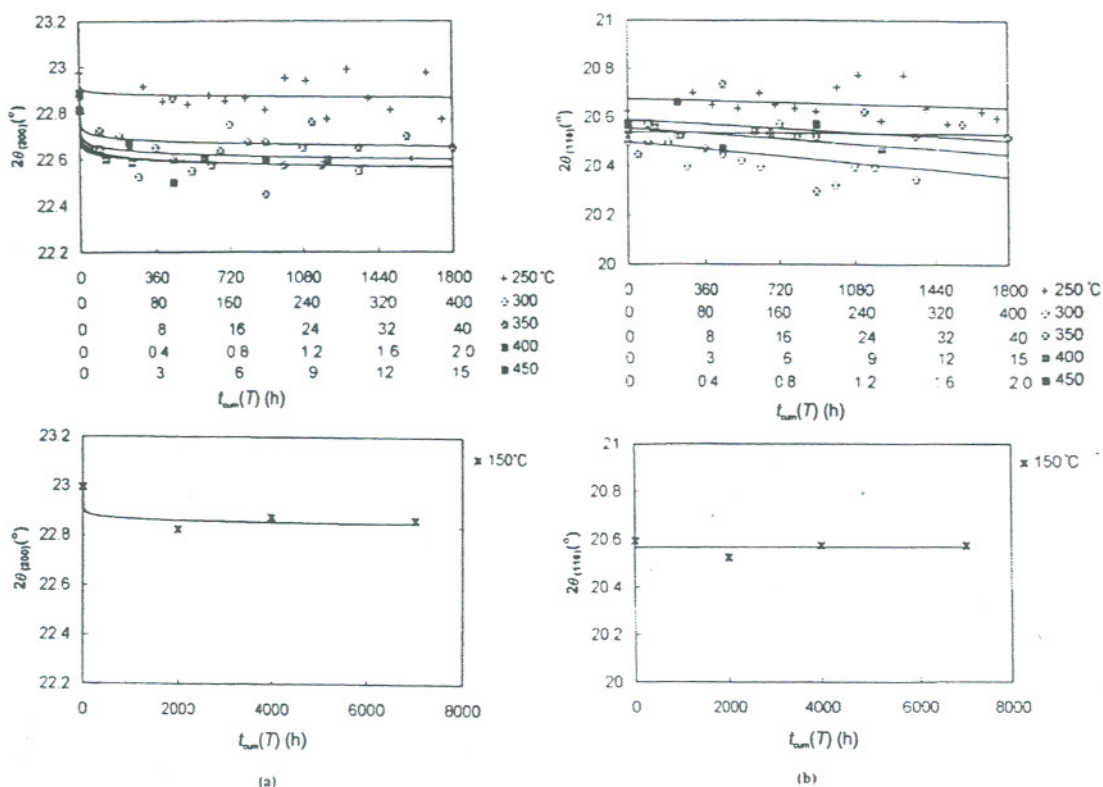


Figure 6. (a) Variation in  $2\theta$  (200) values. (b) Variation in  $2\theta$  (110) values.

time. The major parts of the shifts occur in the early stages of thermal exposures. Figure 6 also depicts the effect of  $T$ . As might be expected, at higher temperatures the shifts are enhanced.

The observed changes in the  $2\theta$  values also exemplify the angular separation  $\Delta(2\theta)$  defined as  $\Delta(2\theta) = 2\theta(200) - 2\theta(110)$ . As the shift in the  $2\theta(200)$  values are more dominant, the curves in figure 7 resemble the trend manifested by the (200) reflection (figure 6). Based on the direct correlation between the tensile strength and the  $2\theta$  values [9] and the data in figure 7, it may be anticipated that the tensile strength drops more in the early stages of aging. Further quantitative evidence for such a drop in the tensile strength will be presented subsequently in this paper.

### 3.1.3. Half width, $\omega$

Fractional variations in the half widths of the equatorial reflections are shown in figure 8. Here,  $\omega_0$  represents the half width value of reflections recorded from samples, prior to heat treatment. The observed changes are significant, with an average  $|\Delta|/\sigma$  value of 3.5. The equatorial reflections from fibers aged at  $T$  values  $< T_d$  tend to sharpen in the early stages of aging and with further continuance of exposure, they begin to broaden. It was also observed that the reflection (110) sharpens more than (200) for all the  $T$  values  $< T_d$ .

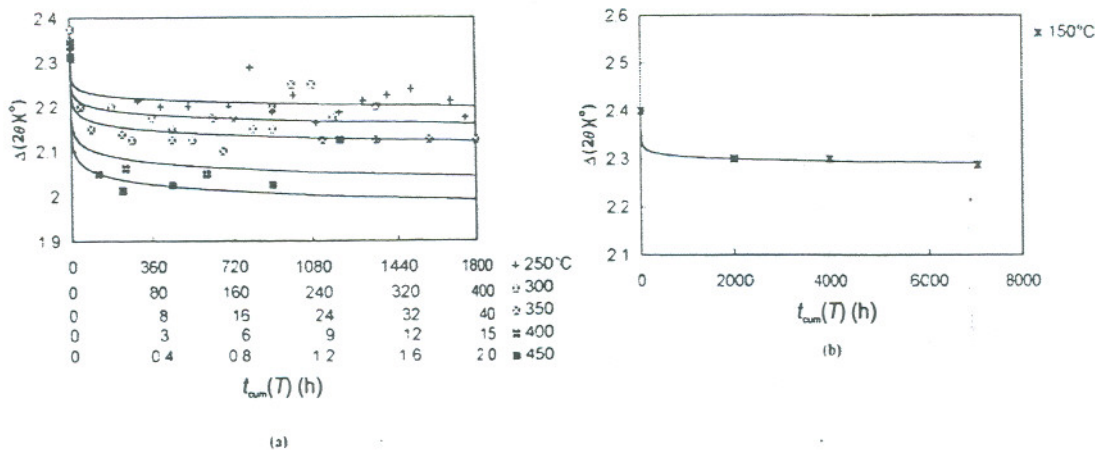


Figure 7.  $\Delta(2\theta)$  values indicating the closing up of basal plane reflections from fibers aged at (a) 250–450 and (b) 150°C.

The duration of the cumulative exposure time over which the reflections remain sharpened is, however, dependent on the  $T$  value. For comparatively high values of  $T$ , the sharpened state is rather short lived. Figure 8(a) shows that at 150°C, even after 7000 h of cumulative exposure, the reflections have not started broadening whereas in contrast, at 250°C, after 1800 h of exposure, broadening has commenced. These features clearly show that at 150°C the fragmentation of crystallites and/or the build-up of micro-strain, which are characteristics of broadening, do not get initiated even up to 7000 h of exposure.

3.1.4. Azimuthal spread,  $\beta$

The alignment of polymer chains is affected by cumulative exposures to  $T$  values  $< T_d$ . Figure 9 provides a comparison of the azimuthal spreads of the equatorial reflections recorded from samples exposed to 150, 250, 300 and 400°C for 7000, 1800, 120 and 15 h, respectively. The misalignment at 150°C is slightly less conspicuous. The increase in the azimuthal spread suggests that the tensile moduli of the corresponding fibers have, perhaps, deteriorated.

3.1.5. Relative intensities

As in the case of 500 and 550°C [3, 5], the relative intensities of the equatorial reflections get affected at all  $T$  values other than 150°C. As can be seen from figure 1, prior to thermal exposure,  $I(200)$  is  $> I(110)$ . With continuing thermal exposures, the peak intensities tend to become equal. The intensity changes may be associated with minor structural changes the details of which are, however, not presently available. X-ray data thus indicate that no significant structural changes are introduced at 150°C even after 7000 h of exposure.



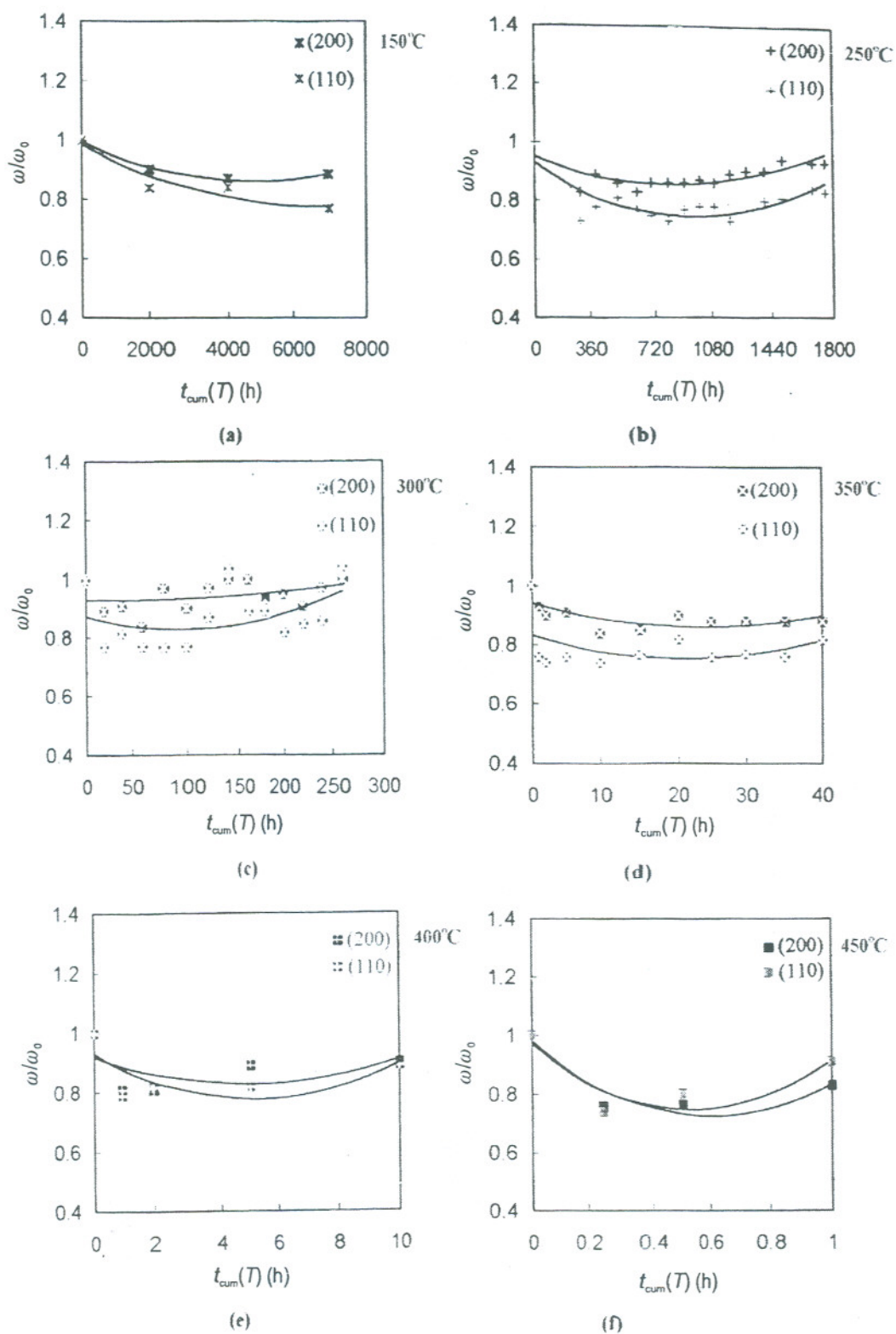


Figure 8. Fractional variation in equatorial half widths for fibers aged at (a) 150 (b) 250 (c) 300 (d) 350 (e) 400 and (f) 450°C.

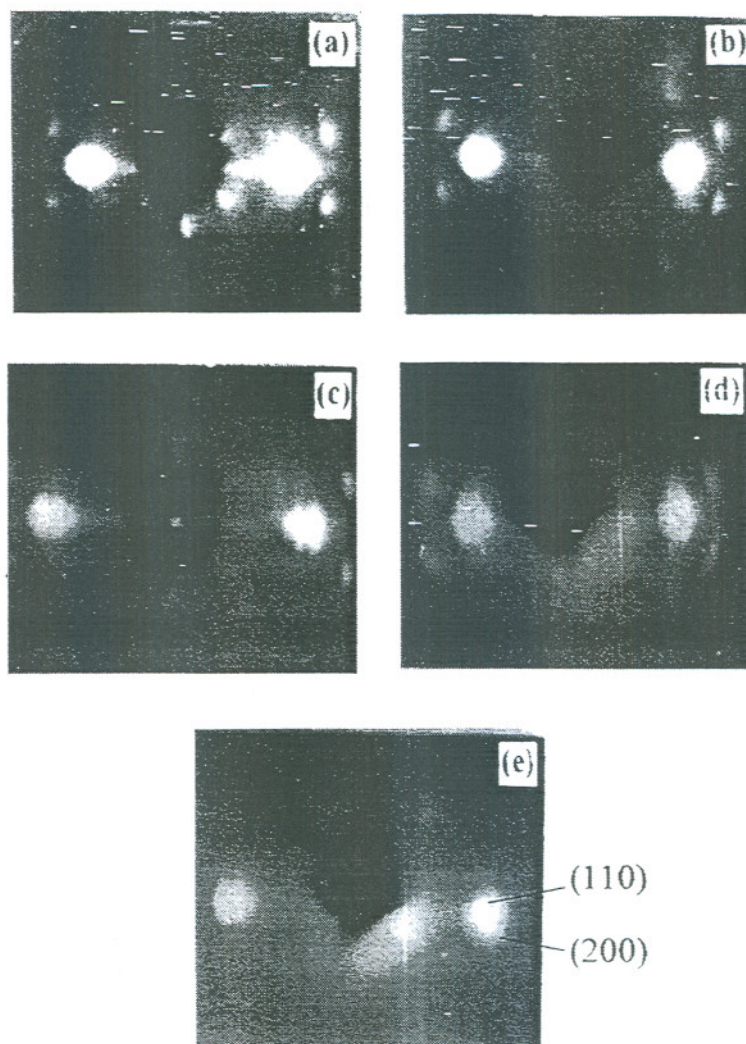


Figure 9. Azimuthal spread of the equatorial reflections (110) and (200). (a) As received; (b) 150°C, 7000 h; (c) 250°C, 1800 h; (d) 300°C, 120 h; and (e) 400°C, 15 h.

X-ray observations presented thus far indicate that the overall nature of changes in the crystal structural characteristics introduced at  $T$  values  $< T_d$  are very similar to those introduced at  $T$  values  $\sim T_d$  [3, 5]. Data corresponding to both  $T$  values  $\sim T_d$  and  $T$  values  $< T_d$ , provide unambiguous evidence that the crystal structural characteristics are influenced by two parameters namely  $T$  and  $t_{\text{cum}}(T)$ . Figure 10 is a schematic representation of a model depicting the changes in the crystal structural characteristics introduced during thermal aging.

### 3.2. Microscopy

Optical and scanning electron microscopic studies show that isothermal aging at  $T$  values  $< T_d$  leads to significant changes in the surface characteristics, the details of which

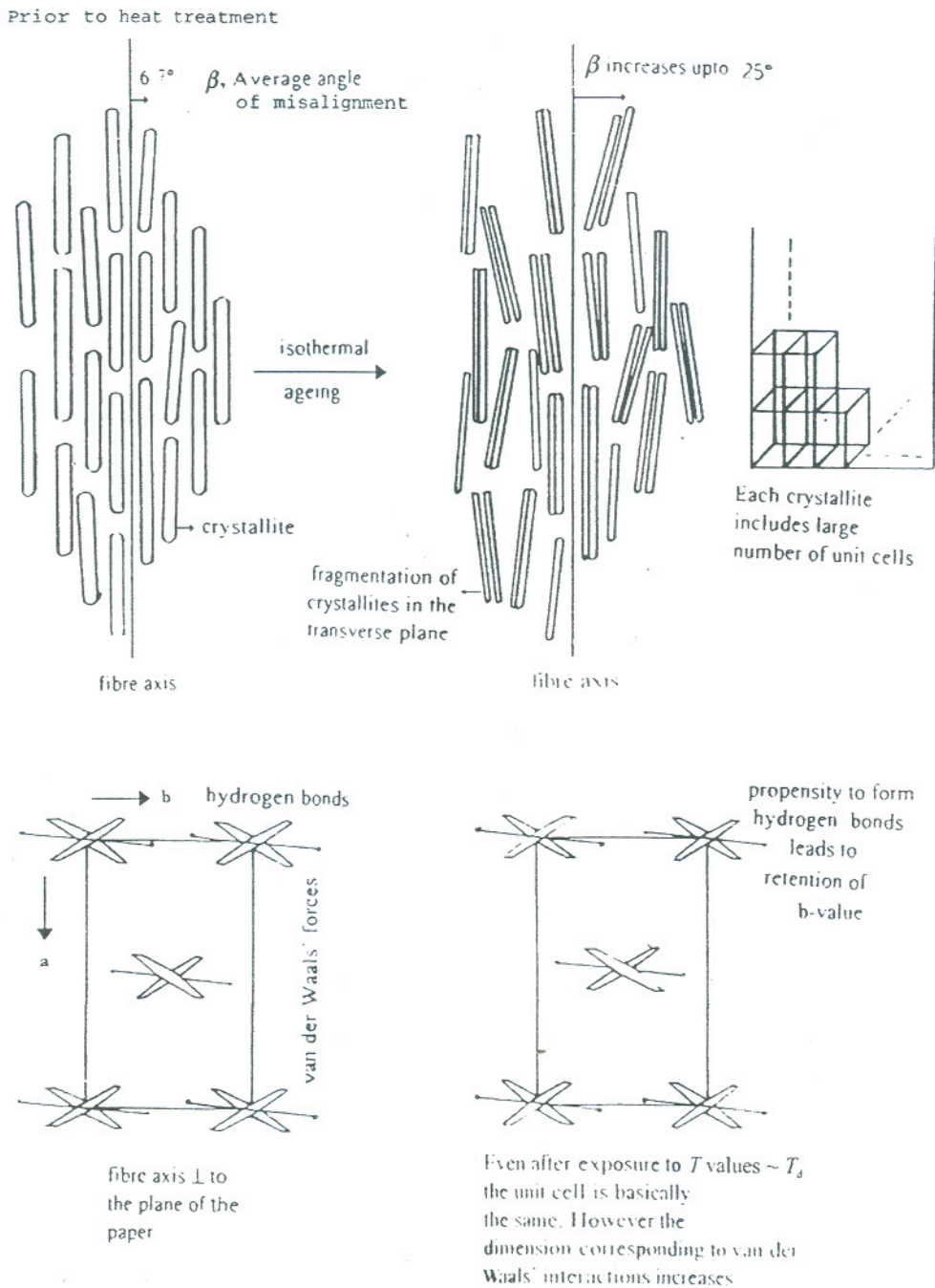


Figure 10. Schematic model depicting changes in the crystal structural characteristics which accompany isothermal aging.

are presented in this section. Some aspects of the cross-section of fractured fibers have also been included.



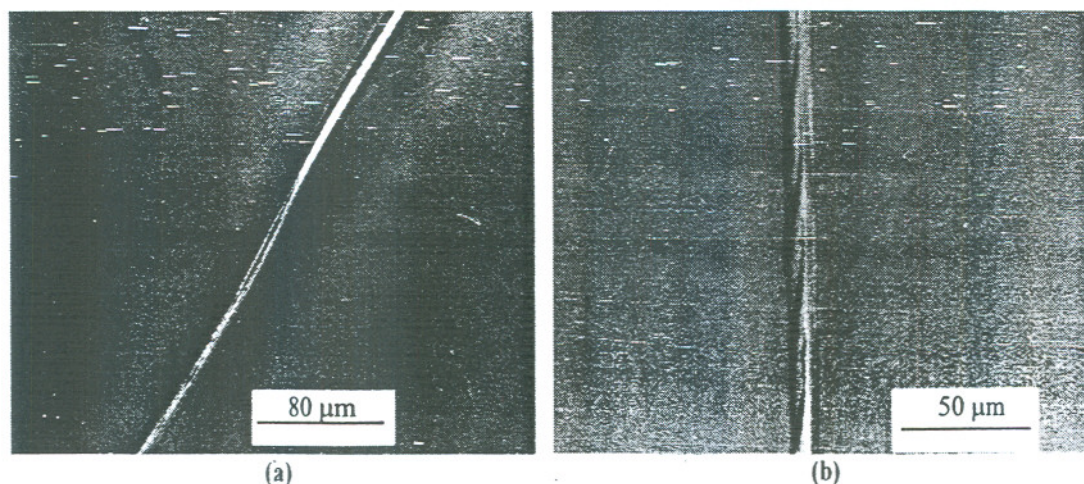


Figure 11. Longitudinal openings on the surface of Kevlar fibers aged at 150°C. Openings (a) parallel and (b) inclined to the fiber axis.

### 3.2.1. Surface characteristics

The most striking features observed on the surface of isothermally aged fibers were as follows:

- (i) introduction of longitudinal openings, groove-like features and peel-offs;
- (ii) formation of holes;
- (iii) introduction of material deposits; and
- (iv) localized loss of material.

As in the case of crystal structural characteristics derived from X-ray data, the above-mentioned macro features are also found to be influenced by two parameters, namely,  $T$  and  $t_{\text{cum}}(T)$ . There follows a description of the surface features described in the order of increasing temperature.

**150°C.** For Kevlar 49 fibers, 150°C is well within the recommended service range of temperatures [10]. Unlike in the case of X-ray data, the surface characteristics of fibers exposed to 150°C for 7000 h manifest striking as well as unwelcome changes. The optical micrographs in figure 11 illustrate the typical surface openings observed in fibers exposed to 150°C for 7000 h. It may be noticed that the orientations of the longitudinal openings with respect to the fiber axis are quite varied. Figure 11(a) depicts an opening nearly parallel to the fiber axis whereas in Figure 11(b), a nearly helical distribution of openings is seen. The introduction of such openings can indeed affect the tensile properties of the fiber and can also facilitate unwanted retention of extraneous material on the surface.

The scanning electron micrograph in figure 12 shows excoriation of the surface of the fiber. When the peel-off is long enough, it tends to wind around the fiber. Such effects can be expected to affect the adhesion between the fiber and the matrix in a composite.

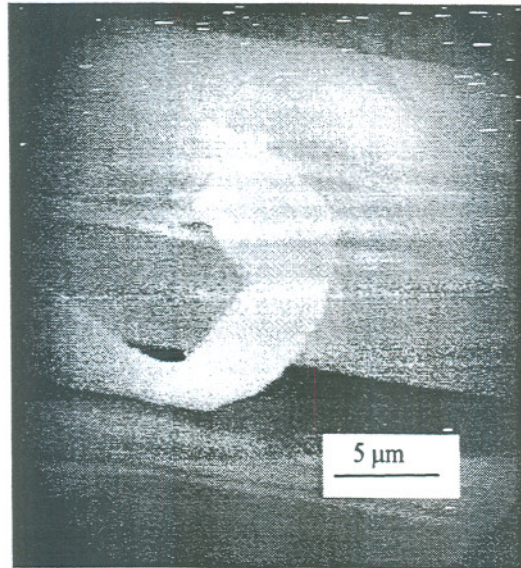


Figure 12. Excoriation of the fiber surface at 150°C.

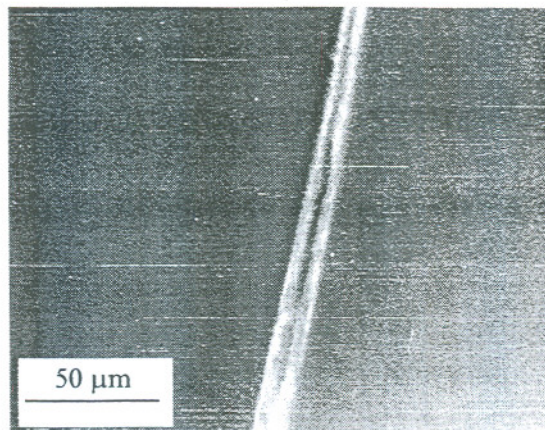


Figure 13. Splitting open of the surface of fibers aged at 250°C.

250°C. For Kevlar, 250°C is also within the recommended service range of temperatures. As in the case of fibers exposed to 150°C, longitudinal openings are found on the surface (figure 13). An additional effect which has been observed concerns the introduction of minute holes (figure 14). The holes, although sparse, are uniformly distributed on the surface. The diameter of the holes ranges from 0.05 to 0.3  $\mu\text{m}$ . In some parts of the surface, very close to the holes, minute quantities of extraneous material has also been found. It is likely that the holes are associated with the evolution of material from within the fiber. No in-situ chemical analysis could be carried out to identify the material on the surface. It must, however, be mentioned that Kalashnik et al.'s mass spectrometric analy-



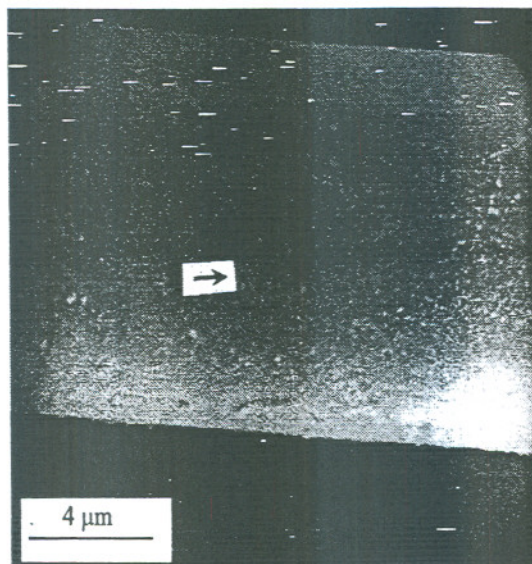


Figure 14. Formation of holes on the surface of fibers aged at 250°C. Arrow shows a typical hole.

sis has enabled chemical identification of materials which evolved at a higher temperature, namely at 510°C [11].

The occurrence of surface holes and extraneous material at  $T$  values as low as 250°C (in comparison with 500 and 550°C, as used in the earlier study [3, 5]) strongly suggests that at this temperature, the prime factor responsible for the introduction of these effects is the duration of cumulative exposure, which in this case was 1800 h. It appears therefore that prolonged exposures to lower temperatures introduce effects similar to those of comparatively short exposures to higher temperatures. As the micrographs were recorded only at selected stages of thermal aging, the introduction of holes cannot be pinpointed precisely on the time scale.

**300°C.** Surface characteristics of fibers exposed to 300°C for 120 and 300 h, respectively, have been examined. As in the case of exposure to 250°C, a longitudinal groove-like feature was found on the surface of fibers exposed to 300°C for 120 h (figure 15). Figure 16 shows the surface holes introduced at 300°C. Yet another type of surface damage resulting from isothermal aging at 300°C is shown in figure 17. A crater-like feature indicating loss of material can be seen. Interestingly, the crater is found beneath a surface impurity. As has been reported by Morgan and Pruneda [12] and Vijayan [13], commercially received Kevlar fibers include detectable amounts of surface impurities. The enhanced degradation of Kevlar fibers at sites close to the impurities suggests that presence of impurities in the as-received fibers can lead to enhanced localized deterioration of the surface, at those specific sites.

The micrograph in figure 18 depicts a localized reduction in fiber thickness. Here, the fiber has lost most of the material which constitutes its thickness. This feature could



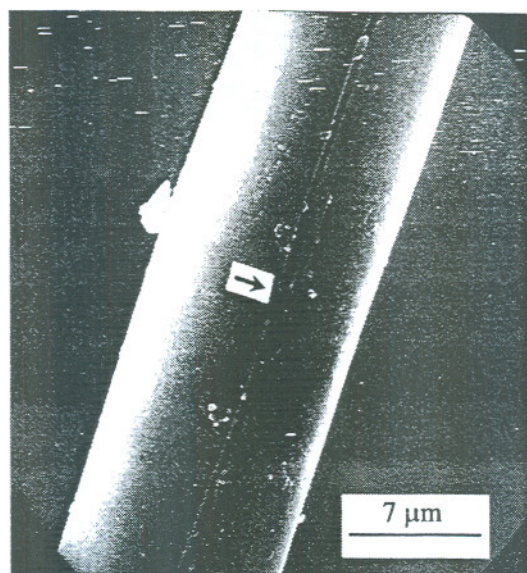


Figure 15. Longitudinal groove (indicated by the arrow) on the surface of fiber heated to 300°C for 120 h.

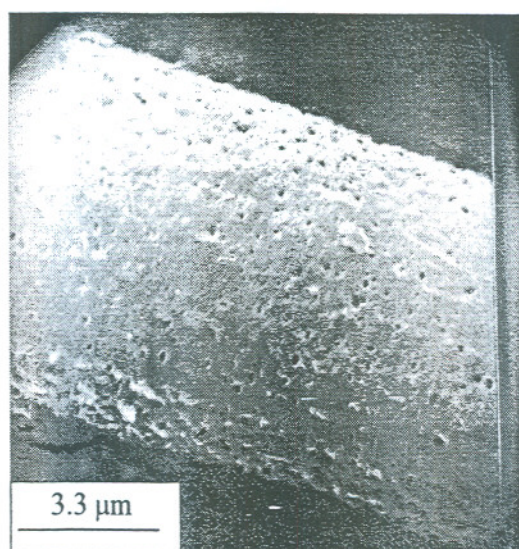


Figure 16. Formation of numerous holes on the surface of fibers heated to 300°C for 300 h.

be considered as a more severe version of the loss of material shown in figure 17. Introduction of such localized damage distributed randomly along the length of the fiber can result in a reduction in the average diameter of the filament which indeed has been experimentally confirmed. Values of the fiber diameter averaged along the length shows that the initial value of 12.2 (38)  $\mu\text{m}$  has decreased by approximately 10%, i.e., to 10.97 (48)  $\mu\text{m}$ .

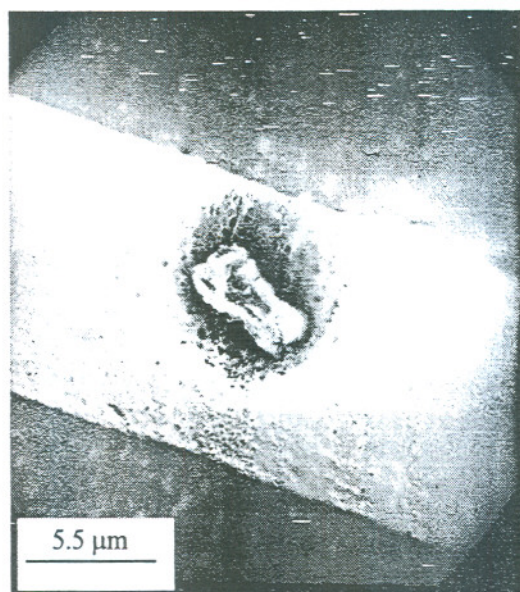


Figure 17. Degradation of surface at site close to an impurity in a fiber aged at 300°C.

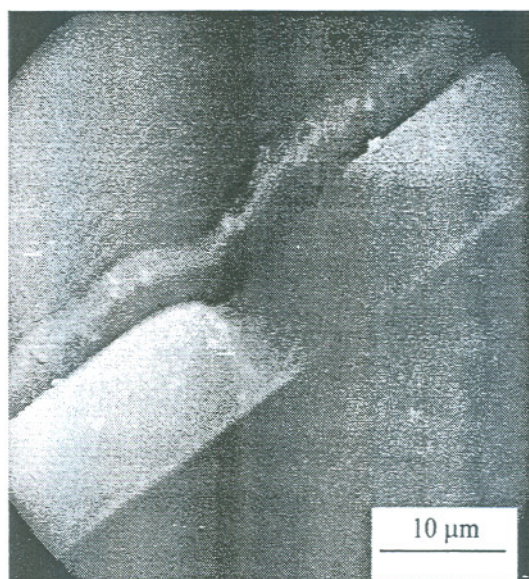
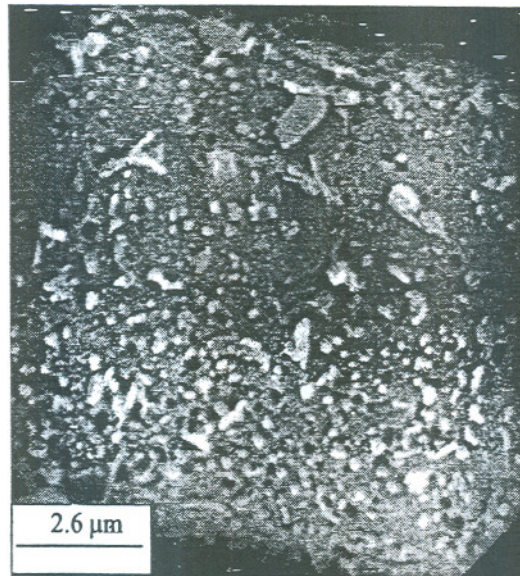


Figure 18. Localised reduction in fiber diameter in a fiber aged at 300°C.

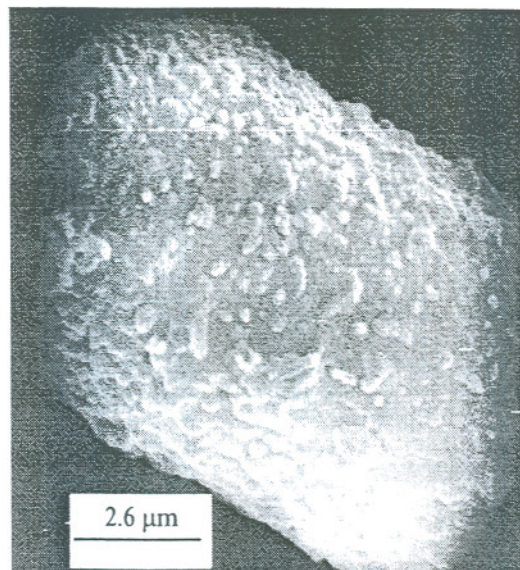
400°C. The most conspicuous surface characteristic of fibers aged at 400°C for 15 h is the introduction of large quantities of extraneous material. The micrographs in figures 19 and 20 show that the surface of fibers exposed to 400°C for 15 h has got nearly completely covered with extraneous material. It may not be presumptuous to assume that the extra material has emerged from within the fiber during heat treatment. The holes in figure 19 support the concept of evolution of material from within the fiber, via the holes.





---

Figure 19. Introduction of large holes on the surface of fibers aged at 400°C for 15 h.



---

Figure 20. Presence of extraneous matter near the surface holes in fibers aged at 400°C for 15 h.

Based on the above-mentioned details on surface characteristics of fibers aged at 150, 250, 300 and 400°C it may be inferred that the peel-offs and the longitudinal grooves appear in the initial stages of aging. Formation of holes and extraneous material on the surface follow subsequently. All the above-mentioned surface characteristics suggest that the initial tensile properties deteriorate with isothermal aging.



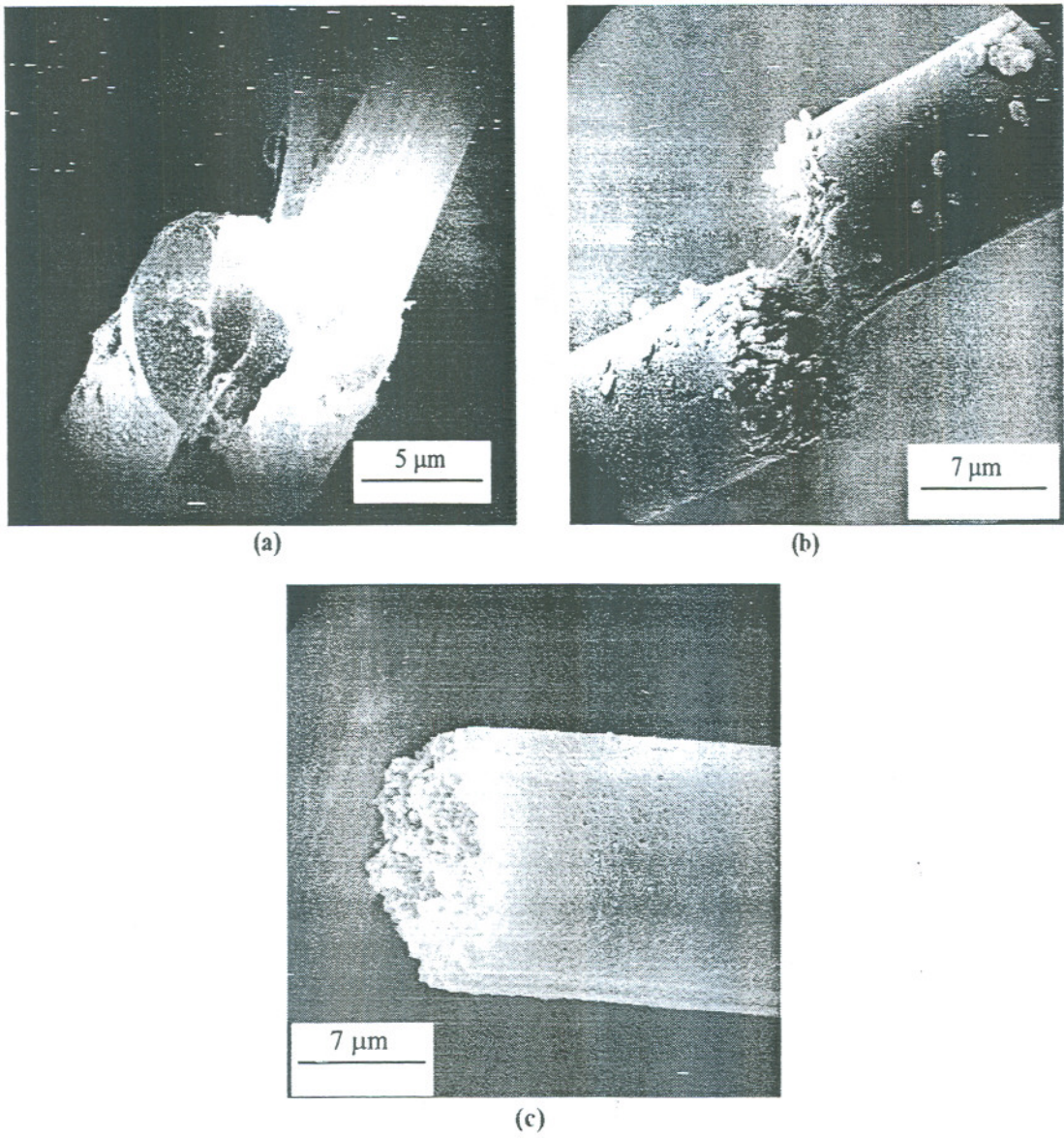


Figure 21. Brittle fracture of fibers aged at (a) 150 (b) 250 and (c) 400°C.

3.2.2. Cross-sectional features

In the case of fibers aged at  $T \sim T_d$ , it was found that in addition to the introduction of surface damages, there was also material loss near the core of the fiber [3, 5]. To find out whether similar features are introduced by aging at  $T$  values  $< T_d$ , the cross-section of fibers fractured in tension have been examined. Figures 21(a)–(c) represent the micrographs from fibers isothermally aged at 150, 250 and 400°C for 7000, 1800 and 15 h, respectively, and fractured in tension. All the three fractures are of the brittle type. Brittle fracture manifested by fibers aged at  $T$  values close to  $T_d$ , is not surprising. Interestingly, the present study provides evidence of brittle fracture by fibers aged at temperatures as

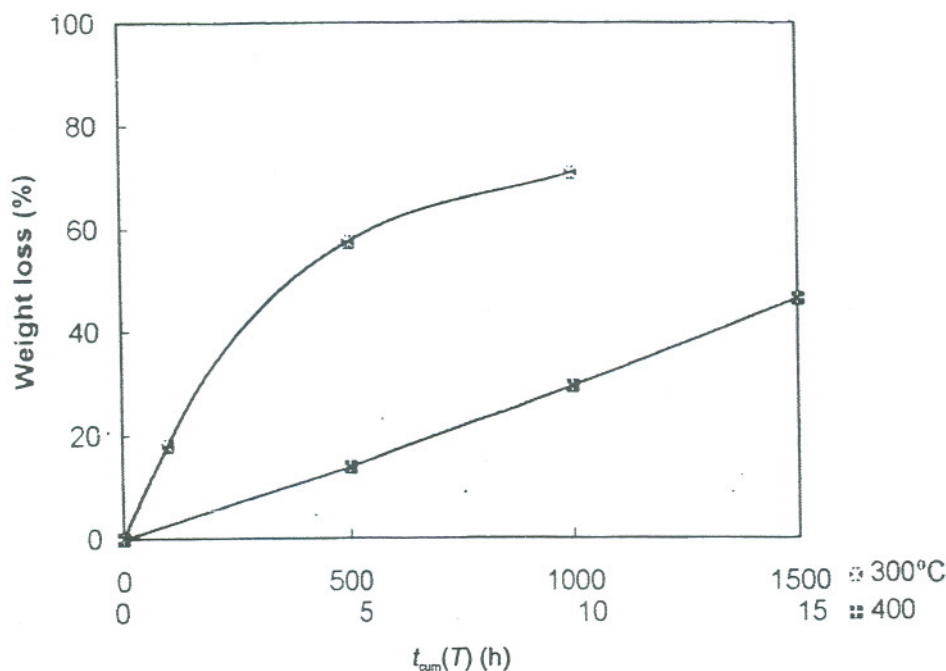


Figure 22. Weight loss manifested by fibers aged at 300 and 400°C.

low as 150°C also. This feature strongly points to the role of the parameter  $t_{cum}(T)$ . Examination of the micrographs in figure 21 further suggests that the fibers aged at 250 and 400°C also tend to get hollow. The degree of hollowness is, however, much less than what was observed at  $T \sim T_d$  [3, 5]. Thus, material loss near the core of the fiber also seems to be a feature common to isothermal aging at both  $T \sim T_d$  and  $T$  values  $< T_d$ .

### 3.3. Weight loss

Fibers exposed to  $T$  values  $< T_d$  manifest weight loss. Figure 22 depicts the weight loss manifested by fibers aged at 300 and 400°C, respectively. All the observed changes in weight are significant, with the average  $|\Delta|/\sigma$  value being 30.9. It was found that after 1000 h at 300°C, the weight loss is  $\sim 70\%$ . Fibers exposed to 250°C for 1800 h show a weight loss of only 6% (not shown in figure 22). In a similar fashion, even after 7000 h of exposure to 150°C, the fibers do not show any weight loss. This feature conforms well with the earlier mentioned observation that the surface of fibers exposed to 150°C do not develop holes even after 7000 h of exposure.

### 3.4. Tensile properties

In the preceding sections, it was shown that aging at  $T$  values  $< T_d$  caused changes in the crystal as well as macro-structural characteristics. These changes indeed suggest al-



Table 1. Tensile characteristics of some of the heat-treated fibers.

Heat treatment conditions [ $T$ ( $^{\circ}\text{C}$ ), $t_{\text{cum}}(T)$ (h)]	Tensile strength (GPa)	Tensile modulus (GPa)
As received	3.25 (16)	107 (6)
150, 7000	1.59 (64)	96 (8)
250, 50	1.92 (58)	109 (8)
250, 1800	0.35 (11)	*
300, 5	2.19 (60)	108 (12)
300, 10	1.69 (30)	115 (7)
300, 20	1.23 (35)	*
300, 30	0.23 (06)	*
400, 1	1.62 (36)	100 (7)

\*Too brittle to be determined.

terations from the initial, exceptional tensile properties of the fiber. Reduction in X-ray crystallinity, broadening of reflections and increase in the azimuthal spread suggest deterioration in the initial tensile modulus. Closing up of the equatorial reflections, weight loss, introduction of hollowness and surface damages suggest reduction in the initial tensile strength. The values of tensile strength and modulus estimated for some of the heat-treated fibers are listed in table 1. The trend manifested by the tensile properties conforms well with the structural changes.

### 3.5. Fifty percent reductions and the order of occurrence of events

Based on the data presented thus far, the duration of exposure,  $t_{0.5}$ , needed for 50% reduction in crystallinity, weight and tensile strength, respectively, have been estimated for various temperatures (figure 23). The relative disposition of the curves suggests the order in which the thermally induced effects occur. It is found that the tensile strength is the most sensitive parameter, followed by crystallinity and then the weight. Comparison of the activation energies for 50% reductions in crystallinity and tensile strength, namely  $105.8 \text{ kJ mol}^{-1}$  (this paper), and  $54 \text{ kJ mol}^{-1}$  [14], respectively, also support the above-mentioned sequence of events. The curves in figure 23 can also be used for predicting the  $t_{0.5}$  values for any intermediate temperature.

### 3.6. The $T$ - $t_{\text{cum}}(T)$ effect

Comparison of the results on fibers exposed to  $T$  values  $\sim T_d$  [3, 5] and  $T$  values  $< T_d$  (this paper) shows that there are many similarities. In both cases, the tensile properties, and particularly the tensile strength decreases, crystallinity reduces, weight losses are introduced, surface damage is incurred, crystallographic parameters change and the fibers eventually suffer decomposition (which is treated synonymous with total loss in crystallinity), at the



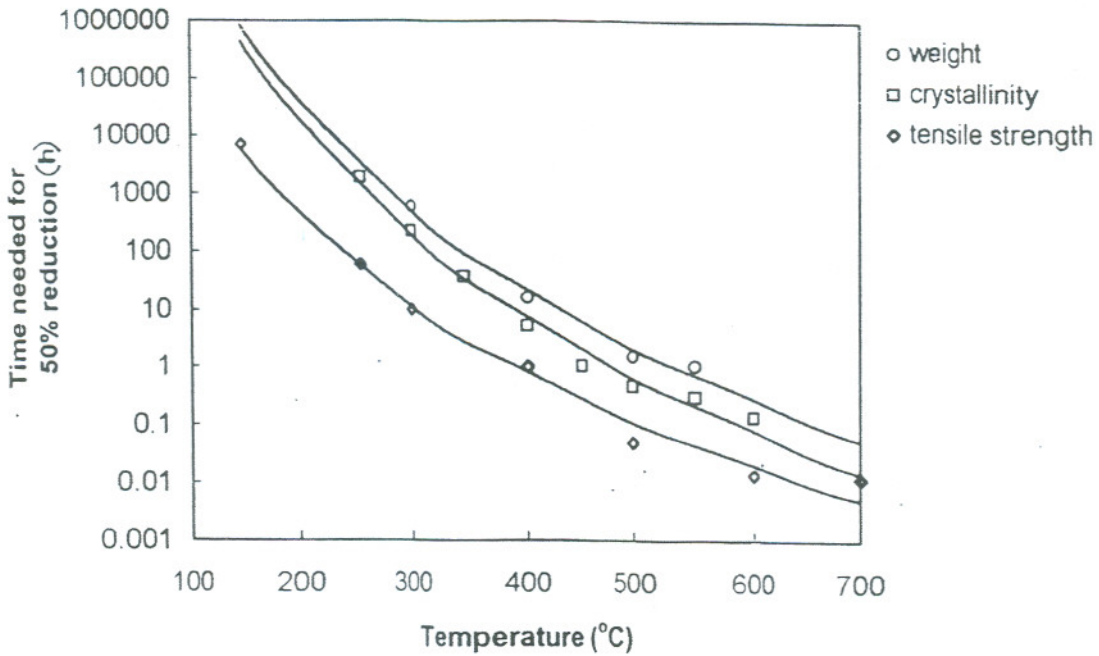


Figure 23. Comparison of time required for 50% reduction in tensile strength, crystallinity and weight. The y-axis is on log scale.

Table 2.  $T$  and  $t_{\text{cum}}(T)$  values corresponding to zero crystallinity.

$T$ (°C)	$t_{\text{cum}}(T)$ (h)
550	0.67
500	1.0
450	3.5
400	16
350	74
300	432
250	> 1800
150	>> 7000

end of prolonged exposure to any chosen temperature. The most conspicuous feature is that changes which occur at a higher temperature  $T_2$  occur at a lower temperature  $T_1$  also when the exposure to the lower temperature  $T_1$  is long enough. Typical examples can be noted from figure 23. A 50% reduction in crystallinity, which occurs after 190 h of exposure to 300°C, recurs at 250°C also when the exposure time is extended to 1460 h. Similarly, a 50% reduction in tensile strength occurs at various temperatures, however, for different values of the cumulative exposure time,  $t_{\text{cum}}(T)$ . Table 2 lists the  $t_{\text{cum}}(T)$  values obtained at various temperatures for reaching the state of zero X-ray crystallinity. As can be seen, at 550°C, 40 minutes of exposure is required to reach the zero crystallinity state

whereas at lower temperatures, the duration of exposure is much more than at 550°C. Thus, the data on isothermally aged Kevlar 49 fibers provide ample evidence that the parameters  $T$  and  $t_{\text{cum}}(T)$  always act in unison.

To sum up, all the thermally induced effects chosen in the present study, are controlled by two parameters, namely  $T$  and  $t_{\text{cum}}(T)$ . Changes which occur at a higher temperature  $T_2$  recur at a lower temperature  $T_1$  also when the exposure to the latter is long enough. This feature is referred to as the  $T$ - $t_{\text{cum}}(T)$  effect.

It must be admitted that the role of the parameter  $t_{\text{cum}}(T)$  controlling the thermally induced effects is not very surprising. The kinetics of any chemical reaction is indeed controlled by the time factor. The interesting observation that has emerged from the present study is that in addition to chemical effects (such as the reactions responsible for the evolution and deposit of materials) the structural features also manifest a dependence on the time factor,  $t_{\text{cum}}(T)$ . In particular, the crystallographic parameters showing an unambiguous dependence on both  $T$  and  $t_{\text{cum}}(T)$  is a hitherto unknown feature.

## 4. CONCLUSIONS

The residual effects of thermal aging at  $T$  values  $< T_d$  are the introduction of crystallographic and macro-structural changes, weight losses and changes in tensile properties. Reduction in tensile strength is shown to precede changes in crystallinity and weight. All the thermally induced effects are controlled by two parameters, namely,  $T$  and  $t_{\text{cum}}(T)$ . The changes which get introduced at  $T$  values  $\sim T_d$  are shown to recur at  $T$  values far below  $T_d$ . The activation energy associated with 50% reduction in initial crystallinity is 105.8 kJ mol<sup>-1</sup>.

*Acknowledgement.* The authors acknowledge the Council of Scientific and Industrial Research (CSIR) of India for sanction of an Emeritus Scientist scheme under which part of the work reported in this paper has been carried out. The authors wish to thank Dr T. A. Bhaskaran and Mr M. A. Venkataswamy for their help in recording the scanning electron micrographs, Mr M. A. Parameswara for his help in recording the optical micrographs. They are grateful to Mr G. Basavaraj and Dr N. Balasubramanian of Everest Building Products for enabling the tensile testing. They acknowledge the support from Dr B. R. Pai, Director, NAL and Dr R. V. Krishnan, Head, Materials Science Division, NAL.

## NOTE

1. Author to whom correspondence should be addressed: e-mail: kvnal@yahoo.com

## REFERENCES

- [1] Tadokoro H 1979 *Structure of Crystalline Polymers* (New York: John Wiley & Sons) p 397
- [2] Yang H H 1989 *Aromatic High Strength Fibres* (New York: John Wiley & Sons) p 191
- [3] Iyer R V and Vijayan K 1999 *Bull. Mater. Sci.* **22** 331
- [4] Jain A and Vijayan K 2003 *High Perform. Polym.* **15** 105



- [5] Iyer R V 1999 *Ph.D. Thesis* Bangalore University, India
- [6] Shioya M, Ojima T and Yamashita J 2001 *Carbon* **39** 1869
- [7] Hindeleh A M and Abdo sh M 1989 *Polymer* **30** 218
- [8] Northolt M G 1974 *Eur. Polym. J.* **10** 799
- [9] Shubha M, Parimala H V and Vijayan K 1991 *J. Mater. Sci. Lett.* **10** 1377
- [10] DuPont Bulletin K-1 1974
- [11] Kalashnik A T, Panikarova N P, Dovbh Ye V, Kozhina G.V, Kalmykova V D and Papkov S P 1978 *Polym. Sci. USSR* **19** 3173
- [12] Morgan R J and Pruneda C O 1987 *Polymer* **28** 340
- [13] Vijayan K 1987 *Curr. Sci.* **56** 1055
- [14] Parimala H V and Vijayan K 1993 *J. Mater. Sci. Lett.* **12** 99